Second virial coefficients for ^{4}He and ^{3}He from an accurate relativistic interaction potential

P. Czachorowski [1,*] M. Przybytek [1] M. Lesiuk [1] M. Puchalski [2] and B. Jeziorski [1]

[1]*Faculty of Chemistry, University of Warsaw, Pasteura 1, 02-093 Warsaw, Poland*
[2]*Faculty of Chemistry, Adam Mickiewicz University, Umultowska 89b, 61-614 Poznań, Poland*

The second virial coefficient and the second acoustic virial coefficient for helium-4 and helium-3 are computed for a wide range of temperatures (0.5–1000 K) using a highly accurate nonrelativistic interaction potential [M. Przybytek *et al.*, Phys. Rev. Lett. **119**, 123401 (2017)] and recalculated relativistic and quantum-electrodynamic components. The effects of the long-range retardation and of the nonadiabatic coupling of the nuclear and electronic motion are also taken into account. The results of our calculations represent at least fivefold improvement in accuracy compared to the previous *ab initio* work. The computed virial coefficients agree well with the most accurate recent measurements but have significantly smaller uncertainty.

I. INTRODUCTION

The existence of physical systems which can be both measured and theoretically described with a good accuracy is invaluable to science. Not only can they help to test the consistency of our understanding of nature, but they may also allow for development of new experimental techniques. For fundamental metrology, helium can be considered such a system. In contrast to hydrogen, seemingly simpler to describe, helium atoms interact particularly weakly. For example, the helium dimer is either weakly bound in its single vibrational state (helium-4) or bound states do not exist at all (helium-3). This allows for accurate calculation of properties of gaseous helium solely in terms of pair interaction potential, as the three- and more-body effects become important only at larger pressures. Due to the simplicity of the system, theoretical description of the helium pair potential can include contributions beyond the Born-Oppenheimer nonrelativistic approximation. Adiabatic, nonadiabatic, relativistic, and quantum-electrodynamic (QED) effects can be added in a systematic manner, if the need arises. The potential can be then used to predict properties of helium such as the energy of the bound state or—crucial in metrology—the second density virial coefficient $B(T)$ and the acoustic virial coefficient $\beta_a(T)$. Accurate knowledge of these coefficients has been exploited by dielectric-constant gas thermometry [1,2], acoustic gas thermometry [3,4], single-pressure refractive-index gas thermometry (SPRIGT) [5,6], and refractive-index gas thermometry [7], as well as utilized in development of new pressure standards [8–10]. At present, the uncertainty of $B(T)$ dominates the uncertainty budget for the electrical measurements of gas pressure at 7 MPa [10] and for the SPRIGT measurements of temperature below 20 K [6]. Thus, one can expect that reducing the error of the pair potential for helium and of the resulting virial coefficients will be

of importance to experimental work in the field of thermal metrology.

The significance of the $B(T)$ coefficient is best seen from the form of the virial equation of state,

$$p = k_{\mathrm{B}}T[\rho + B(T)\rho^2 + \cdots], \tag{1}$$

used in accurate determination of the thermodynamic temperature T, pressure p, or, until 2019, the Boltzmann constant (fixed exactly at $k_{\mathrm{B}} = 1.380\,649 \times 10^{-23}$ J/K by the 2018 revision of the International System of Units [11]). The density ρ can be determined from electrical measurements using the Clausius-Mossotti equation [12]

$$\frac{\varepsilon_r - 1}{\varepsilon_r + 2} = \frac{4\pi}{3}\alpha_{\mathrm{d}}[\rho + b_\varepsilon(T)\rho^2 + \cdots], \tag{2}$$

where ε_r is the relative electric permittivity, α_{d} is the atomic dipole polarizability, and $b_\varepsilon(T)$ is the second dielectric virial coefficient.

Eliminating ρ from Eqs. (1) and (2), one can express the pressure through ε_r:

$$p = \frac{k_{\mathrm{B}}T}{4\pi\alpha_{\mathrm{d}}}(\varepsilon_r - 1) + \frac{k_{\mathrm{B}}T}{16\pi^2\alpha_{\mathrm{d}}^2}$$
$$\times \left[B(T) - b_\varepsilon(T) - \frac{4\pi}{3}\alpha_{\mathrm{d}}\right](\varepsilon_r - 1)^2 + \cdots, \tag{3}$$

with the relative error of the order of $(\varepsilon_r - 1)^2$. This error can be further reduced to $(\varepsilon_r - 1)^3$ if the third virial coefficient $C(T)$ and the third dielectric virial coefficient $c_\varepsilon(T)$ are included in Eqs. (1) and (2), respectively. An equation similar to Eq. (3) holds if ρ is measured optically and p is expressed via the index of refraction $n = (\varepsilon_r\mu_r)^{1/2}$, μ_r being the magnetic permeability. The major difference would be that the denominator in the first term of Eq. (3) would be replaced by $2\pi(\alpha_{\mathrm{d}} + \chi_{\mathrm{m}})$, where χ_{m} is the magnetic susceptibility related to μ_r via $\mu_r = 1 + 4\pi\chi_{\mathrm{m}}\rho$. Since χ_{m} is much smaller than α_{d} and $b_\varepsilon(T)$ is significantly smaller than $B(T)$, the major factors

---

*Corresponding author: pczachor@chem.uw.edu.pl

determining the accuracy of Eq. (3) and its optical variant are the accuracy of the polarizability α_d and of the second virial coefficient $B(T)$.

In this paper we report accurate theoretical determination of $B(T)$ and of the second acoustic virial coefficient $\beta_a(T)$ for gaseous helium-4 and helium-3 within the wide temperature range 0.5–1000 K. We also present an improved helium pair interaction potential which can be used in calculations of other thermophysical properties of gaseous helium or properties of the helium dimer itself.

II. THEORY

A. Second virial coefficient

The second virial coefficient $B(T)$ can be conveniently expressed in terms of one- and two-atomic partition functions Z_1 and Z_2 [13]:

$$B(T) = -\mathcal{V}\left(Z_2 - \tfrac{1}{2}Z_1^2\right)/Z_1^2, \qquad (4)$$

where $\mathcal{V}$ is the volume of the system. After inserting explicit forms of Z_1 and Z_2 [14] into Eq. (4), $B(T)$ can be partitioned into three distinct parts [15]:

$$B(T) = B_{\text{ideal}}(T) + B_{\text{bound}}(T) + B_{\text{th}}(T), \qquad (5)$$

where $B_{\text{ideal}}(T)$ is the ideal gas contribution, $B_{\text{bound}}(T)$ is the effect contributed by bound rovibrational states of the dimer, and $B_{\text{th}}(T)$ is the "thermal contribution," dependent on the scattering dimer states. For a monatomic, bosonic gas, these contributions are defined as [15]

$$B_{\text{ideal}}(T) = -\frac{1}{16}\frac{1}{2s+1}\Lambda^3(T), \qquad (6)$$

$$
\begin{aligned}
B_{\text{bound}}(T) = -\Lambda^3(T) \\
\times \Bigg\{ \sum_{v,l}^{l\,\text{even}}(2l+1)\frac{s+1}{2s+1}\left(e^{-E_{v,l}/(k_B T)}-1\right) \\
+ \sum_{v,l}^{l\,\text{odd}}(2l+1)\frac{s}{2s+1}\left(e^{-E_{v,l}/(k_B T)}-1\right)\Bigg\},
\end{aligned}
\qquad (7)
$$

$$B_{\text{th}}(T) = -\frac{\Lambda^3(T)}{\pi k_B T}\int_0^\infty dE\; e^{-E/(k_B T)}\mathcal{S}(E), \qquad (8)$$

where v and l in the summations in Eq. (7) run over quantum numbers (vibrational and rotational, respectively) of the bound states of the system, $E_{v,l}$ are energies of these bound states, and s is the spin of the nucleus. Furthermore,

$$\Lambda(T) = \sqrt{2}\lambda_B = \frac{h}{\sqrt{2\pi\mu_a k_B T}}, \qquad (9)$$

$$
\begin{aligned}
\mathcal{S}(E) = \sum_{l\,\text{even}}^{\infty}(2l+1)\frac{s+1}{2s+1}\delta_l(E) \\
+ \sum_{l\,\text{odd}}^{\infty}(2l+1)\frac{s}{2s+1}\delta_l(E),
\end{aligned}
\qquad (10)
$$

where λ_B is the thermal de Broglie wavelength, h is the Planck constant, $\mu_a = m_a/2$ is the reduced mass of two atoms, and $\delta_l(E)$ are phase shifts for the energy E and the angular momentum quantum number l. For helium-4, $s = 0$ and there

is one bound state, $E_{0,0}$, which has to be taken into account in Eq. (7). For fermionic gases, such as ^{3}He ($s = 1/2$), B_{ideal} changes sign, and the s-dependent prefactors (spin weights) in the expressions for $B_{\text{bound}}(T)$ and for $\mathcal{S}(E)$ are interchanged [14]. There are no bound rovibrational states of the helium-3 dimer, so for that isotope one has $B_{\text{bound}}(T) = 0$.

With the values of $B(T)$ calculated for a suitable range of temperatures T, one can easily obtain the second acoustic virial coefficient $\beta_a(T)$ [15]:

$$
\begin{aligned}
\beta_a(T) = 2B(T) + 2(\gamma_0 - 1)T\frac{dB(T)}{dT} \\
+ \frac{(\gamma_0 - 1)^2}{\gamma_0}T^2\frac{d^2 B(T)}{dT^2},
\end{aligned}
\qquad (11)
$$

where γ_0 is the heat capacity ratio ($\gamma_0 = 5/3$ for a monatomic gas with three degrees of freedom). The differentiation of $B(T)$ is straightforward and can be done analytically using Eqs. (5)–(10).

B. Schrödinger equation

To calculate $B_{\text{bound}}(T)$ and $B_{\text{th}}(T)$, the Schrödinger equation for the dimer has to be solved to determine the energy of the bound state of ^{4}He$_2$ and the phase shifts. In the center-of-mass frame, with the origin in the geometric center of the nuclei, the equation for a binuclear molecule takes the form

$$(H_{\text{el}} + H_n - E)\Psi(\boldsymbol{r},\boldsymbol{R}) = 0, \qquad (12)$$

where

$$H_{\text{el}} = -\frac{1}{2}\sum_i \nabla_{\boldsymbol{r}_i}^2 - \sum_i \frac{Z_A}{r_{iA}} - \sum_i \frac{Z_B}{r_{iB}} + \sum_{i<j}\frac{1}{r_{ij}} + \frac{Z_A Z_B}{R}, \qquad (13)$$

$$H_n = -\frac{1}{2\mu_n}\left(\nabla_{\boldsymbol{R}}^2 + \nabla_{\text{el}}^2\right) + \left(\frac{1}{M_A} - \frac{1}{M_B}\right)\boldsymbol{\nabla}_{\text{el}}\boldsymbol{\nabla}_{\boldsymbol{R}}, \qquad (14)$$

where the indices i, j denote the electrons, $\boldsymbol{\nabla}_{\text{el}} = \frac{1}{2}\sum_i \boldsymbol{\nabla}_{\boldsymbol{r}_i}$, $\boldsymbol{r}$ denote all electronic coordinates $\boldsymbol{r}_i$ collectively, A and B denote the nuclei, M_A and M_B are the nuclear masses, $\mu_n = M_A M_B/(M_A + M_B)$ is the reduced nuclear mass, Z_A and Z_B are the nuclear charges, and $\boldsymbol{R} = \boldsymbol{R}_A - \boldsymbol{R}_B$ is a vector connecting the nuclei. We are interested in homonuclear molecules only, so the rightmost term in Eq. (14) vanishes. Note that in this section, as well as further on, we use atomic units (reduced Planck constant $\hbar$, elementary charge e, Bohr radius a_0, and electron mass m_e are used as units of action, electric charge, length, and mass, respectively), unless stated otherwise.

To describe the finite-nuclear-mass effects, we employed the nonadiabatic perturbation theory (NAPT) of Pachucki and Komasa [16,17]. It assumes the wave function in the form

$$\Psi(\boldsymbol{r},\boldsymbol{R}) = \psi(\boldsymbol{r};\boldsymbol{R})Y_l^m(\theta,\phi)\chi_l(R)/R + \delta\Psi_{\text{na}}(\boldsymbol{r},\boldsymbol{R}), \qquad (15)$$

where $Y_l^m(\theta,\phi)$ is a spherical harmonic. It is assumed that $\langle\delta\Psi_{\text{na}}|\psi\rangle_{\text{el}} = 0$, where the symbol $\langle\cdot|\cdot\rangle_{\text{el}}$ denotes integration over the electronic coordinates only. The function $\psi(\boldsymbol{r};\boldsymbol{R})$ depends parametrically on $\boldsymbol{R}$ and is a solution of the electronic Schrödinger equation (with fixed nuclear positions)

$$H_{\text{el}}(\boldsymbol{R})\psi(\boldsymbol{r};\boldsymbol{R}) = \mathcal{E}(R)\psi(\boldsymbol{r};\boldsymbol{R}). \qquad (16)$$

In the leading NAPT order, the equation for the nuclear wave function $\chi_l(R)$ is

$$\left[-\frac{1}{2\mu_\mathrm{n}}\frac{d^2}{dR^2}+\frac{l(l+1)}{2\mu_\mathrm{n}R^2}+V(R)-E\right]\chi_l(R)=0. \quad (17)$$

The potential $V(R)$ depends on the level of theory. In the simplest case, in the nonrelativistic Born-Oppenheimer (BO) approximation, $V(R)=V_\mathrm{BO}(R)\equiv\mathcal{E}(R)$. A detailed description of the potential used in our calculation is given in the next section.

While the adiabatic, relativistic, and QED corrections can be taken into account just by including a proper term in $V(R)$, the nonadiabatic effects require further modifications of Eq. (17) itself. When the finite-nuclear-mass effects up to $(m_\mathrm{e}/\mu_\mathrm{n})^2$ order are included in the Hamiltonian, the nuclear wave function $\chi_l(R)$ can be evaluated from [17]

$$\left[-\frac{1}{2\mu_\parallel(R)}\frac{d^2}{dR^2}-\frac{d\mathcal{W}_\parallel(R)}{dR}\frac{d}{dR}+\frac{d\mathcal{W}_\parallel(R)}{dR}\frac{1}{R}\right.$$
$$\left.+\frac{l(l+1)}{2\mu_\perp(R)R^2}+V(R)+V_\mathrm{na}(R)-E\right]\chi_l(R)=0, \quad (18)$$

with

$$\frac{1}{2\mu_{\perp/\parallel}(R)}=\frac{1}{2\mu_\mathrm{n}}+\mathcal{W}_{\perp/\parallel}(R), \quad (19)$$

where the potential $V(R)$ contains at least the BO and adiabatic contributions. The most significant change from Eq. (17) is the appearance of the "distance-dependent masses" in place of the reduced nuclear mass. The functions $\mathcal{W}_\parallel(R)$, $\mathcal{W}_\perp(R)$, and $V_\mathrm{na}(R)$ take nonadiabatic effects into account and are defined in Ref. [17], the last one denoted there as $\delta\mathcal{E}_\mathrm{na}(R)$. In fact, it is more convenient to use them with their value for the separated atoms limit subtracted [17,18]. Then

$$\frac{1}{2\mu_{\perp/\parallel}(R)}=\frac{1}{2\mu_\mathrm{a}}+\mathcal{W}_{\perp/\parallel}^\mathrm{int}(R)+O\left(\frac{1}{\mu_\mathrm{n}^3}\right), \quad (20)$$

$$\mathcal{W}_{\perp/\parallel}^\mathrm{int}(R)=\mathcal{W}_{\perp/\parallel}(R)-\mathcal{W}_{\perp/\parallel}(\infty), \quad (21)$$

$$V_\mathrm{na}^\mathrm{int}(R)=V_\mathrm{na}(R)-V_\mathrm{na}(\infty), \quad (22)$$

where $\mu_\mathrm{a}=\mu_\mathrm{n}+1$. For the specific case of He$_2$, these functions were calculated in Ref. [18].

C. Phase shifts

As the internuclear distance R increases, the wave function of the interacting atoms approaches that of free particles and can be written as [19]

$$\chi_l(R)\sim R[j_l(kR)-n_l(kR)\tan\delta_l(E)], \quad (23)$$

where $k=\sqrt{2\mu_\mathrm{a}E}$ and the symbols $j_l(x)$ and $n_l(x)$ denote the spherical Bessel and Neumann functions, respectively. By employing this expression, the phase shifts can be calculated as [19]

$$\delta_l(E)=\lim_{R\to\infty}\delta_l(E,R), \quad (24)$$

$$\tan\delta_l(E,R)=\frac{kj_l'(kR)-\gamma_l(R)j_l(kR)}{kn_l'(kR)-\gamma_l(R)n_l(kR)}, \quad (25)$$

$$\gamma_l(R)=\frac{\chi_l'(R)}{\chi_l(R)}-\frac{1}{R}. \quad (26)$$

From a numerical standpoint, the above procedure can be repeated for increasing R and stopped when the apparent shift function $\delta_l(E,R)$ converges to an acceptable level.

Note that Eq. (25) allows to calculate the phase shift only up to a multiple of π. There are different methods to give it an absolute value, for example, by defining the shift for zero or infinite energy and exploiting its continuity to obtain it for other energies, leaning on semiclassical expressions, or even employing an alternative formula which provides an intrinsically absolute shift (compare, e.g., Ref. [20]). In our calculations, we require that $\delta_l(E)=0$ for a free particle [$V(R)\equiv0$]. As a result, for a repulsive potential one has $\delta_l(E)<0$, whereas for an attractive interaction $\delta_l(E)>0$ [19]. Moreover, when $E\to0$ for a fixed potential $V(R)$, the value of the phase shift tends to $n_l\pi$, where n_l is the number of bound states supported by the potential for given angular momentum quantum number l—the behavior known from the Levinson theorem [19,21]. Additionally, we require that the apparent shift $\delta_l(E,0)=0$ and then ensure that it is a continuous function of R during calculation [20].

III. PAIR POTENTIAL FOR THE HELIUM DIMER

Following the approach used previously in Refs. [22] and [18], we represent the interaction energy of a pair of helium atoms as a sum of the BO potential, $V_\mathrm{BO}(R)$, and a set of corrections that account for major post-BO effects: the leading-order coupling of the nuclear and electronic motion, known as the adiabatic correction, $V_\mathrm{ad}(R)$, the relativistic, $V_\mathrm{rel}(R)$, and QED effects, $V_\mathrm{QED}(R)$:

$$V(R)=V_\mathrm{BO}(R)+V_\mathrm{ad}(R)+V_\mathrm{rel}(R)+V_\mathrm{QED}(R). \quad (27)$$

All components of $V(R)$ for a given internuclear distance R were obtained using the supermolecular approach by computing the difference between the respective dimer and atomic contributions

$$V_\mathrm{Y}(R)=\Delta E_\mathrm{Y}=E_\mathrm{Y}-2E_\mathrm{Y}^A, \quad (28)$$

where Y $=$ BO, ad, rel, QED. E_BO is the nonrelativistic BO energy of the helium dimer. E_ad is formally defined as the expectation value of the nuclear kinetic energy operator [23]. Therefore, calculation of E_ad requires differentiation of the clamped-nuclei wave function of the dimer with respect to nuclear coordinates, on which the wave function depends parametrically. E_ad can be calculated using various methods [16,24–28]. In Refs. [22,29], the Born-Handy approach [24–26] was used, while the results of Ref. [18] were obtained with the method proposed by Pachucki and Komasa [16]. E_Y, Y $=$ rel, QED, are formally defined as expectation values of the operators $\hat{H}_\mathrm{Y}$, shown below, corresponding to a particular physical effect and computed with the nonrelativistic electronic BO function. The atomic contributions, E_Y^A, Y $=$ BO, ad, rel, QED, are defined similarly, but correspond to a single helium atom.

The operator $\hat{H}_\mathrm{rel}$ is the Breit-Pauli Hamiltonian [30], which for closed-shell systems in a singlet state consists of the mass-velocity operator $\hat{H}_\mathrm{mv}$, the one- and two-electron Darwin

operators $\hat{H}_{D1}$ and $\hat{H}_{D2}$, and the Breit operator $\hat{H}_{Br}$:

$$\hat{H}_{rel} = \hat{H}_{mv} + \hat{H}_{D1} + \hat{H}_{D2} + \hat{H}_{Br}, \qquad (29)$$

where

$$\hat{H}_{mv} = -\frac{1}{8}\alpha^2 \sum_i p_i^4, \qquad (30)$$

$$\hat{H}_{D1} = \frac{\pi}{2}\alpha^2 \sum_I \sum_i Z_I \delta(\boldsymbol{r}_i - \boldsymbol{r}_I), \qquad (31)$$

$$\hat{H}_{D2} = \pi\alpha^2 \sum_{i<j} \delta(\boldsymbol{r}_{ij}), \qquad (32)$$

$$\hat{H}_{Br} = -\frac{1}{2}\alpha^2 \sum_{i<j} \left[\frac{\boldsymbol{p}_i \cdot \boldsymbol{p}_j}{r_{ij}} + \frac{\boldsymbol{r}_{ij} \cdot (\boldsymbol{r}_{ij} \cdot \boldsymbol{p}_j)\boldsymbol{p}_i}{r_{ij}^3} \right]. \qquad (33)$$

In these equations, $\boldsymbol{r}_{ij} = \boldsymbol{r}_i - \boldsymbol{r}_j$, $\boldsymbol{p}_i = -i\nabla_{\boldsymbol{r}_i}$, the index I runs over all the nuclei, with charge Z_I and located at the position $\boldsymbol{r}_I$, $\delta(\boldsymbol{r})$ is the Dirac delta function, and $\alpha = 1/137.035\,999\,084$ is the fine structure constant [11]. The sum of one-electron operators is usually referred to as the Cowan-Griffin (CG) operator [31], $\hat{H}_{CG} = \hat{H}_{mv} + \hat{H}_{D1}$.

The operator $\hat{H}_{QED}$, defining the QED correction, can be expressed as the linear combination

$$\hat{H}_{QED} = \frac{8\alpha}{3\pi}\left(\frac{19}{30} - 2\ln\alpha - \ln k_0\right)\hat{H}_{D1}$$
$$+ \frac{\alpha}{\pi}\left(\frac{164}{15} + \frac{14}{3}\ln\alpha\right)\hat{H}_{D2} + \hat{H}_{AS}, \qquad (34)$$

of $\hat{H}_{D1}$, $\hat{H}_{D2}$ and the Araki-Sucher (AS) operator $\hat{H}_{AS}$ [32–34] defined as

$$\hat{H}_{AS} = -\frac{7}{6\pi}\alpha^3 \sum_{i<j} \hat{P}(r_{ij}^{-3}), \qquad (35)$$

where $\hat{P}(r_{ij}^{-3})$ is the operator distribution

$$\langle \hat{P}(r_{ij}^{-3}) \rangle = \lim_{a\to 0} \langle r_{ij}^{-3}\theta(r_{ij} - a) + 4\pi(\gamma + \ln a)\delta(\boldsymbol{r}_{ij}) \rangle, \quad (36)$$

with $\theta(r)$ and γ standing here for the Heaviside step function and the Euler-Mascheroni constant, respectively. The quantity $\ln k_0$ in Eq. (34) is the so-called Bethe logarithm [30]. The interatomic distance dependence of $\ln k_0$ is weak [35], especially for a weakly interacting system such as the helium dimer [22], and can be neglected at the accuracy level considered in this work. Therefore, we fixed $\ln k_0$ at its helium atom value equal to $4.370\,160\,222\,0(1)$ [36].

In the present work, the values of all four components of $V(R)$ in Eq. (27) were obtained for a set of 55 distances ranging from 1 to 30 bohrs. The recommended BO interaction energies for 46 distances, $1 \leqslant R \leqslant 9$ bohrs, and the adiabatic corrections for a full set of distances were taken from Ref. [18] together with their estimated theoretical uncertainties. The remaining data points—the BO energies at nine distances, $10 \leqslant R \leqslant 30$ bohrs, and the relativistic and QED corrections—were recalculated using a Gaussian orbital approach with larger one-electron basis sets than the ones employed in Ref. [18]. The new calculations revealed that theoretical uncertainties of some components of $V_{rel}(R)$ estimated in Ref. [18] were too optimistic so they were carefully reexamined in the present work. The AS interaction energies were calculated initially in

Ref. [22] (for 17 interatomic distances only) using explicitly correlated Gaussian (ECG) expansion of the wave function for the dimer and near exact atomic AS energy [37]. Due to the basis set superposition error (BSSE), they had absolute uncertainties of virtually the same magnitude for all $R \geqslant 5$ bohrs. As a result, the AS correction was the dominant source of theoretical error of the pair potential $V(R)$ for large distances.

The BO energies (at $10 \leqslant R \leqslant 30$ bohrs) and the expectation values of the operators constituting the relativistic correction, Eqs. (30)–(33), were evaluated at two levels of theory: the coupled-cluster method with single, double, and noniterative triple excitations [CCSD(T)], and the full configuration interaction (FCI) method. Note that the calculations at the CCSD(T) level were performed utilizing the Hellman-Feynman theorem, according to the linear response theory [38]. The individual interaction energies were then obtained using a two-step procedure as the following sum:

$$\Delta E_Y = \Delta E_Y^{CCSD(T)} + \delta E_Y^{FCI}, \qquad (37)$$

where $Y = BO$, mv, D_1, D_2, Br. The first, dominating term $\Delta E_Y^{CCSD(T)}$ is defined by Eq. (28) and the much smaller FCI correction δE_Y^{FCI} is defined as

$$\delta E_Y^{FCI} = \Delta E_Y^{FCI} - \Delta E_Y^{CCSD(T)} \qquad (38)$$

with the quantities on the right-hand side of Eq. (38) computed using the same basis set.

The AS correction, defined by the operator in Eq. (35), was determined only at the FCI level:

$$\Delta E_{AS} = \Delta E_{AS}^{FCI}. \qquad (39)$$

When computing $\Delta E_Y^{CCSD(T)}$ and ΔE_Y^{FCI} via Eq. (28), the atomic properties E_Y^A were obtained with the corresponding dimer-centered basis set, which is equivalent to using the so-called counterpoise scheme, which corrects for BSSE [39]. All calculations were performed using modified dXZ basis sets of Ref. [22] (containing 21 uncontracted s functions) with the cardinal numbers X up to $X = 8$ for CCSD(T) and up to $X = 7$ for FCI. The largest FCI calculations employed a wave function with approximately 2×10^9 determinants (at D_{2h} symmetry). The CCSD(T) calculations were performed using the DALTON 2013 package [40,41], whereas at the FCI level we used a program [42] written specifically for the purpose of the present project. In the latter case, the Hartree-Fock orbitals, the standard one- and two-electron integrals, and integrals involving the relativistic operators were generated using the local version of the DALTON 2.0 package [38,40,43], while integrals involving the AS operator were computed using the computer code developed in Ref. [44].

To reduce the basis set incompleteness errors in the quantities obtained from the Gaussian orbital calculations, we employed the Riemann extrapolation scheme introduced in Ref. [45]. This method assumes that the differences $\delta_X = E_X - E_{X-1}$, where E_X are the quantities of interest calculated within a basis set of cardinal number X, behave asymptotically as $\delta_X \sim \text{const} \times X^{-n}$ for $X \to \infty$. As shown in Ref. [45], this leads to the following two-point formula for

the complete basis set (CBS) limit:

$$E_\infty = E_X + X^n(E_X - E_{X-1})\left[\zeta(n) - \sum_{i=1}^X i^{-n}\right], \qquad (40)$$

where $\zeta(s) = \sum_{i=1}^\infty i^{-s}$ is the Riemann zeta function. In the case of the Born-Oppenheimer potential, we used $n = 4$ in the above formula. The same scheme was found to be adequate for the mass-velocity and one-electron Darwin corrections. However, the remaining contributions to the total potential have a different convergence rate. In the case of the two-electron Darwin correction we employed $n = 2$, in agreement with the analytic results of Kutzelnigg [46] for the helium atom. The Breit correction was extrapolated with $n = 5/2$ as suggested by the previous numerical results for He$_2$ [22] [using $\zeta(5/2) \approx 1.34149$]. To apply the Riemann extrapolation to the AS correction, the method presented in Ref. [45] has to be extended because the quantities δ_X behave asymptotically as $\delta_X \sim aX^{-2}\ln X + bX^{-2}$, where a and b are numerical constants (see Ref. [44]). Combining results from three consecutive basis sets, we find the following expression for the CBS limit in this case:

$$E_\infty = E_X + a\left[-\zeta'(2) - \sum_{i=1}^X i^{-2}\ln i\right] + b\left[\zeta(2) - \sum_{i=1}^X i^{-2}\right], \qquad (41)$$

where $\zeta'(s)$ is the derivative of the Riemann zeta function [$\zeta'(2) \approx -0.937548$]. The constants a and b are found from the expressions

$$a = [X^2(E_X - E_{X-1}) - (X - 1)^2(E_{X-1} - E_{X-2})]$$
$$\times [\ln(X) - \ln(X - 1)]^{-1}, \qquad (42)$$

$$b = a\ln X - X^2(E_X - E_{X-1}). \qquad (43)$$

To demonstrate the efficacy of the Riemann extrapolation of the AS correction, one can make a comparison with the ECG results of Cencek *et al.* [22]. At the distance $R = 2.0$ a.u. the ECG result $-0.032\,25(25)$ mK is accurate enough to be treated as a reference. The values obtained using three largest Gaussian orbital basis sets ($X = 5, 6, 7$) are equal to $-0.028\,50$, $-0.028\,88$, and $-0.029\,18$ mK, respectively, and converge rather slowly. The Riemann extrapolation yields $-0.032\,23$ mK, in good agreement with the ECG value. In the attractive part of the potential, the ECG results became inaccurate due to the lack of a BSSE correction, so the Riemann-extrapolated results are much more accurate in this region.

For each quantity considered in this work, the CCSD(T) results, $\Delta E_Y^{\mathrm{CCSD(T)}}$, and the FCI correction, $\delta E_Y^{\mathrm{FCI}}$, were extrapolated separately. The sole exception is the AS correction, where only the FCI results are available and thus were extrapolated directly. The errors of the extrapolated quantities were assigned as follows. In the case of the mass-velocity and one-electron Darwin corrections the extrapolation error is conservatively estimated as a difference between the extrapolated result and the value obtained in the largest basis set available. For the remaining three corrections, this straightforward approach is not adequate since it leads to a gross

overestimation of error. To circumvent this problem, we introduce a modified procedure where the difference between the extrapolated result and the value obtained in the largest basis set is scaled by a constant (independent of the internuclear distance) to get the error estimate. We found that the scaling by a factor of 0.1 is adequate for the two-electron Darwin and AS corrections, while 0.5 is used for the Breit correction. This approach is validated by comparing with the ECG results [22] at short interatomic distances—where the ECG approach is reliable and gives small uncertainties. For example, at $R = 2.0$ a.u. we obtained 1.121(11), 1.944(5), and $-0.0322(3)$ for the two-electron Darwin, Breit, and AS corrections, respectively, after scaling the errors, while the corresponding ECG results read 1.132(5), 1.9411(1), and $-0.0322(3)$. Clearly, the two sets of results are in full agreement and a similar picture is obtained for other interatomic distances where the ECG results are still reliable. For all corrections other than the AS, the errors of the CCSD(T) and FCI contributions were added quadratically to obtain the final error estimates.

To ensure high accuracy of the pair potential for large interatomic distances R, we recalculated the constants $C_n(\mathrm{Y})$, $n < 8$, $\mathrm{Y} = \mathrm{ad, rel, QED}$, determining the leading-order terms in the asymptotic expansion in powers of $1/R$ of the post-BO terms in Eq. (27), $V_Y(R) \sim -\sum_n C_n(\mathrm{Y})/R^n$. The coefficients $C_n(\mathrm{rel})$ and $C_n(\mathrm{QED})$ are defined as appropriate combinations of the coefficients calculated separately for the components of $\hat{H}_{\mathrm{rel}}$ and $\hat{H}_{\mathrm{QED}}$ according to Eqs. (29) and (34). Following Ref. [22], we distinguish between contributions to $C_n(\mathrm{Y})$, $\mathrm{Y} = \mathrm{mv, D1, D2, Br, AS}$, coming from either the intra- or intermonomer part of a given operator $\hat{H}_\mathrm{Y}$. The asymptotic expansion of the intramonomer part always starts with the term proportional to $1/R^6$ and the corresponding coefficient expressed in the sum-over-states form is [22]

$$C_6(\mathrm{Y}, \mathrm{intra}) = -12\sum_{abc}\frac{Z_{0a}Z_{0b}Z_{0c}^2 Y_{ab}}{(\omega_a + \omega_c)(\omega_b + \omega_c)}$$
$$-24\sum_{abc}\frac{Z_{0a}Z_{ab}Z_{0c}^2 Y_{0b}}{(\omega_a + \omega_c)\omega_b}. \qquad (44)$$

The matrix elements Z_{ab} and Y_{ab} are

$$Z_{ab} = \langle\phi_a|\sum_{i=1}^2 z_i|\phi_b\rangle, \qquad (45)$$

$$Y_{ab} = \langle\phi_a|\hat{H}_Y^A|\phi_b\rangle - \delta_{ab}\langle\phi_0|\hat{H}_Y^A|\phi_0\rangle, \qquad (46)$$

where $\hat{H}_Y^A$ are the operators from Eqs. (30)–(33) and (35) defined for a single helium atom, ϕ_0 is the ground-state wave function of helium, ϕ_a are the wave functions of the excited states, and ω_a are the corresponding excitation energies. As it was shown in Ref. [47], the leading-order coefficient for the adiabatic correction, $C_6(\mathrm{ad})$, can be calculated using the same formula, Eq. (44), and in this case the $\hat{H}_{\mathrm{ad}}^A$ operator has the form

$$\hat{H}_{\mathrm{ad}}^A = \frac{1}{2M}\left(\sum_{i=1}^2 \boldsymbol{p}_i\right)^2, \qquad (47)$$

where $M = 7294.299\,541\,42(24)$ [11] is the mass of the helium-4 atom nucleus. Only the two-electron operators,

Eqs. (32), (33), and (35), have an intermonomer part and, among them, only the Breit and AS operators give contributions to the interaction energy that vanish for large distances as powers of $1/R$ [22]. For the Breit interaction, the leading-order coefficients are [22,48]

$$C_4(\text{Br, inter}) = 2 \sum_{ab} \frac{Z_{0a}P_{0a} Z_{0b}P_{0b}}{\omega_a + \omega_b}, \quad (48)$$

$$C_6(\text{Br, inter}) = 18 \sum_{ab} \frac{Z_{0a}P_{0a} Q_{0b}S_{0b}}{\omega_a + \omega_b} - \frac{12}{5} \sum_{ab} \frac{Z_{0a}P_{0a} Z_{0b}T_{0b}}{\omega_a + \omega_b}, \quad (49)$$

where

$$Q_{0a} = \langle \phi_0 | \sum_{i=1}^{2} \frac{1}{2}(3z_i^2 - r_i^2) | \phi_a \rangle, \quad (50)$$

$$P_{0a} = \langle \phi_0 | \sum_{i=1}^{2} p_{zi} | \phi_a \rangle, \quad (51)$$

$$S_{0a} = \langle \phi_0 | \sum_{i=1}^{2} z_i p_{zi} | \phi_a \rangle, \quad (52)$$

$$T_{0a} = \langle \phi_0 | \sum_{i=1}^{2} [2r_i^2 p_{zi} - z_i(\mathbf{r}_i \cdot \mathbf{p}_i)] | \phi_a \rangle. \quad (53)$$

For the AS interaction, the odd-n coefficients up to $n = 7$ are determined exclusively by the expectation value of the intermonomer part of $\hat{H}_{\text{AS}}$ calculated with the product of ground-state wave functions of both interacting atoms. Utilizing multipole expansion of the r_{ij}^{-3} operator [49], it is easy to show that

$$C_3(\text{AS, inter}) = \frac{7}{6\pi} \alpha^3 R_0^2, \quad (54)$$

$$C_5(\text{AS, inter}) = \frac{7}{3\pi} \alpha^3 R_0 R_1, \quad (55)$$

$$C_7(\text{AS, inter}) = \frac{7}{9\pi} \alpha^3 (3R_0 R_2 + 5R_1^2), \quad (56)$$

where

$$R_n = \langle \phi_0 | \sum_{i=1}^{2} r_i^{2n} | \phi_0 \rangle. \quad (57)$$

The C_n and R_n coefficients, Eqs. (44), (48), (49), and (57), were calculated using ECG expansions of the wave functions of a helium atom with $N_b = 128, 256,$ and 512 terms for ϕ_0 and $2N_b$ terms for the excited states ϕ_a in intermediate summations. The values presented in Table I were obtained by taking the results calculated with $N_b = 512$ as the recommended values with their uncertainties estimated as the absolute difference between the $N_b = 256$ and $N_b = 512$ results. The reliability of this procedure was checked by computing the leading-order coefficient in the asymptotic expansion of the V_{BO} potential. The obtained value $C_6(\text{BO}) = 1.460\,977\,837\,723\,6(2)$ agrees to all significant digits with the value $C_6(\text{BO}) = 1.460\,977\,837\,725(2)$ taken from the literature [50] but is somewhat more accurate. The final results for $C_n(Y), n < 8, Y = $ ad, rel, QED, calculated using data from

TABLE I. Components of the leading asymptotic constants of $V_{\text{ad}}(R)$, $V_{\text{rel}}(R)$, and $V_{\text{QED}}(R)$. The labels "intra" and "inter" were omitted, when a given C_n has only one contribution of either type.

$2M_N C_6(\text{ad})$	16.699 662 17(5)
$\alpha^{-2} C_6(\text{mv})$	−31.628 828(6)
$\alpha^{-2} C_6(\text{D1})$	26.786 047(3)
$\alpha^{-2} C_6(\text{D2})$	1.934 254 7(6)
$\alpha^{-2} C_4(\text{Br})$	−0.663 309 369 557 98(6)
$\alpha^{-2} C_6(\text{Br, intra})$	−0.954 535 671(6)
$\alpha^{-2} C_6(\text{Br, inter})$	−2.603 188 510 963(6)
$\alpha^{-3} C_6(\text{AS})$	−1.409 909(1)
R_1	2.386 965 990 037 8(1)
R_2	7.947 129 863 325(1)

Table I agree with the ones used in Ref. [22] but have two to three times more significant digits.

The extrapolated values of $V_{\text{BO}}(R)$, $V_{\text{ad}}(R)$, $V_{\text{rel}}(R)$, and $V_{\text{QED}}(R)$ were fitted separately to the analytic functions of the form

$$\sum_{k=1}^{M} e^{-a_k R} \sum_{i=I_0}^{I_1} P_{ik} R^i - \sum_{n=N_0}^{N_1} f_n(\eta R) \frac{C_n}{R^n}, \quad (58)$$

where $f_n(x) = 1 - e^{-x}(\sum_{i=0}^{n} x^i/i!)$ is the Tang-Toennies damping function [51], a_k, P_{ik}, and η are adjustable parameters, and the summation limits $[M, I_0, I_1, N_0, N_1]$ are $[3, -1, 2, 6, 16]$ for $V_{\text{BO}}(R)$, $[3, 0, 2, 6, 10]$ for $V_{\text{ad}}(R)$, $[2, 0, 2, 4, 10]$ for $V_{\text{rel}}(R)$, and $[3, 0, 2, 3, 10]$ for $V_{\text{QED}}(R)$. The asymptotic constants C_8 and C_{10} for $V_{\text{rel}}(R)$ and $V_{\text{QED}}(R)$ are not known and were adjusted. In both cases C_9 was neglected. The remaining constants C_n were fixed and set equal to the values known from the literature [47,50,52,53] or to the values calculated in this work as described above. In the analytical fitting of $V_{\text{BO}}(R)$, the linear parameters P_{ik} were constrained by imposing the condition

$$V_{\text{BO}}(R) = \frac{4}{R} + (E_{\text{Be}} - 2E_{\text{He}}) + O(R^2) \quad (59)$$

that ensures the correct short-range asymptotics of the potential. The known accurate ground-state energies of the beryllium and helium atoms, $E_{\text{Be}} = -14.667356498$ [54] and $E_{\text{He}} = -2.903724377$ [55], were used. Similarly, the analytical fits of the post-BO corrections were constrained to ensure correct values of the potentials at $R = 0$. The corresponding conditions, $V_{\text{ad}}(0) = 0.0001971680204$, $V_{\text{rel}}(0) = -0.00215235927$, and $V_{\text{QED}}(0) = 0.00039644284$, were obtained using data from Ref. [54] for the berylliumlike united atom, and from Refs. [37,55] for the helium atom. In all cases, the inverse squares of the uncertainties σ were used as the weighting factors to ensure that the fit accuracy is higher in regions of more accurate data points. The average absolute errors of the fits are 0.18σ for $V_{\text{BO}}(R)$, 0.13σ for $V_{\text{ad}}(R)$, 0.15σ for $V_{\text{rel}}(R)$, and 0.13σ for $V_{\text{QED}}(R)$. In some cases, the fitted data points are reproduced with errors that are greater than the estimated data point uncertainties. This behavior was observed only for $R = 26$ and 30 bohrs. For such large distances the values of the potentials are small and their accurate prediction using the supermolecular approach is difficult due to large cancellation of significant digits between

the dimer and atomic contributions in Eq. (28). On the other hand, in this region the potentials are entirely determined by their asymptotic expansion. Therefore, the analytic functions that include an accurate asymptotic constant C_n are expected to provide more reliable results than the ones calculated from Eq. (28).

In order to estimate the uncertainties of physical properties of helium calculated with the present potential, we constructed functions $\sigma_Y(R)$, Y = BO, ad, rel, QED, representing estimated uncertainties of the components $V_Y(R)$ of the interaction potential, such that the exact values of a given component can be assumed to be contained between functions $V_Y(R) \pm \sigma_Y(R)$. The functions $\sigma_Y(R)$ are not intended to accurately reproduce the estimated uncertainties but to follow general trends in their R dependence and to bound most values from above. Analytic functions $\sigma_Y(R)$ used to represent the uncertainties have the general form

$$s_0 e^{-a_0 R} + \sum_{i=1}^{n} s_i e^{-a_i R^2}, \qquad (60)$$

where a_i and s_i are adjustable parameters, and the summation limit n is 4 for $\sigma_{BO}(R)$, and 3 for $\sigma_{ad}(R)$, $\sigma_{rel}(R)$, and $\sigma_{QED}(R)$. The fit of uncertainties was performed using the standard least-squares method applied to a reduced set of data points obtained by discarding points where the values of uncertainties are significantly smaller than the neighboring ones. The value of a_0 was adjusted only once, while constructing the function $\sigma_{BO}(R)$, and then set fixed during generation of the remaining functions. The average ratio of the value of $\sigma_Y(R)$ to the value of estimated uncertainty calculated for a whole set of 55 distances is 1.33 for $\sigma_{BO}(R)$, 1.81 for $\sigma_{ad}(R)$, 1.00 for $\sigma_{rel}(R)$, and 1.04 for $\sigma_{QED}(R)$.

The values of all parameters of the functions $V_Y(R)$ and $\sigma_Y(R)$ (Y = BO, ad, rel, QED), and a numerical implementation of the fits in the form of a FORTRAN 2003 code can be found in the Supplemental Material [56].

The effects of retardation (see Ref. [57] for their precise definition) were included in the potential $V(R)$ using the procedure employed in Ref. [22]. In the retardation damping function $g(x) = (1 + \sum_{n=1}^{5} A_n x^n)/(1 + \sum_{n=1}^{6} B_n x^n)$, the coefficients B_n were taken from Ref. [22], while A_n were recalculated using Eqs. (48)–(52) from the same reference, to conform to more accurate values of the asymptotic constants calculated in the present work.

To conclude this section, let us summarize the improvements that have been made in the description of the helium pair potential since 2012 [22]. The most important achievement is a consistent reduction of errors of the dominant BO component for all distances by about one order of magnitude (4–23 times) done in Ref. [18]. In the case of post-BO corrections, the estimated uncertainties of the present potentials are similar to the ones from Ref. [22] in the highly repulsive region of $V(R)$ for $R \leqslant 3$ and smaller for larger distances. This reduction is by one to two orders of magnitude (7–222 times) for the adiabatic correction and by a factor of about 5 for the relativistic correction. The most significant changes are observed for the QED components where, due to a proper removal of BSSE in the AS term, the ratio of errors estimated in Ref. [22] to the present ones grows steeply from 1.4 at

$R = 3.5$ to 5×10^3 at $R = 12$. Besides reducing the theoretical errors, we were also able to calculate the potential on a much finer grid of points (55 compared to 17 in Ref. [22]) and to improve the description of the long-range decay of post-BO corrections where both the number of terms included in their asymptotic expansion in powers of $1/R$ and the precision of the asymptotic constants were increased. All these factors combined allowed us to produce a more robust and reliable analytical representation of $V(R)$ and its uncertainties $\sigma(R)$ that are needed in the determination of thermophysical properties of helium.

IV. NUMERICAL CALCULATIONS OF SECOND VIRIAL COEFFICIENT

The nonadiabatic nuclear Schrödinger Eq. (18) has the form

$$\left[\frac{d^2}{dR^2} + p(R)\frac{d}{dR} + q(R) \right] f(R) = 0, \qquad (61)$$

with

$$f(R) \equiv \chi_l(R), \qquad (62)$$

$$p(R) \equiv 2\mu_\parallel(R)\frac{d\mathcal{W}_\parallel^{int}(R)}{dR}, \qquad (63)$$

$$q(R) \equiv 2\mu_\parallel(R)\Bigg[E - V(R) - V_{na}^{int}(R)$$

$$- \frac{1}{R}\frac{d\mathcal{W}_\parallel^{int}(R)}{dR} - \frac{l(l+1)}{2\mu_\perp(R)R^2} \Bigg]. \qquad (64)$$

A standard approach to finding a solution of such an equation is the Numerov method [58,59]. However, in the standard formulation of this method there is no first derivative present in the equation. To cast Eq. (61) into the required form, a substitution can be used [60] to remove the problematic first-derivative term

$$f(R) = \phi(R)e^{-\int dR\, p(R)/2}. \qquad (65)$$

This leads to the equation

$$\left[\frac{d^2}{dR^2} + Q(R) \right] \phi(R) = 0, \qquad (66)$$

where

$$Q(R) \equiv q(R) - \frac{1}{4}p^2(R) - \frac{1}{2}\frac{dp(R)}{dR}, \qquad (67)$$

which can now be solved by the Numerov method, using the three-term recurrence

$$(1 - T_{n+1})\phi_{n+1} - (2 + 10T_n)\phi_n + (1 - T_{n-1})\phi_{n-1} = 0, \qquad (68)$$

where $T_n = -Q_n(\Delta R)^2/12$, ΔR is the integration step length, and the subscript n denotes the quantity at the nth integration point. In fact, we employed a slightly modified variant of the method—the so-called renormalized Numerov [61]. If we define

$$F_n = (1 - T_n)\phi_n, \qquad (69)$$

$$U_n = \frac{2 + 10T_n}{1 - T_n}, \qquad (70)$$

and insert it to Eq. (68), one multiplication less per step is needed. The most important point in the renormalized Numerov method, however, is another substitution

$$\mathcal{R}_n = F_{n+1}/F_n, \tag{71}$$

which leads to a two-term recurrence formula

$$\mathcal{R}_n = U_n - \mathcal{R}_{n-1}^{-1}. \tag{72}$$

A benefit of Eq. (72) is that $\mathcal{R}_n$—in contrast to F_n—does not grow exponentially in the classically forbidden regions [61]. The initial value equivalent to $\phi_0 = 0$ and $\phi_1 \neq 0$ is $\mathcal{R}_0 = \infty$ which leads to $\mathcal{R}_1 = U_1$. The two-term formula is obtained from a three-term one for the price of forfeiting the information about the normalization of the wave function. However, in this case it is not needed anyway; only a logarithmic derivative of the function is needed in Eq. (26). It can be expressed as [59,61]

$$[\phi(R)^{-1}d\phi(R)/dR]_{R=R_n}$$
$$= \left(\frac{1/2 - T_{n+1}}{1 - T_{n+1}}\mathcal{R}_n - \frac{1/2 - T_{n-1}}{1 - T_{n-1}}\mathcal{R}_{n-1}^{-1}\right)\frac{1 - T_n}{\Delta R}, \quad (73)$$

and

$$\chi(R_n)^{-1}\frac{d\chi(R)}{dR}\bigg|_{R=R_n} = \phi(R_n)^{-1}\frac{d\phi(R)}{dR}\bigg|_{R=R_n} - \frac{1}{2}p(R_n). \tag{74}$$

As described in Ref. [61], this method can be also adapted easily to calculate energies of the bound states of the system, needed to obtain $B_{\text{bound}}(T)$ in Eq. (7) for helium-4.

In practical application, we chose 250 values of the energy E, distributed logarithmically in the range from 1×10^{-11} to 1 hartree. Although the domain of integration in Eq. (8) is unbounded, the selected range of energies was entirely sufficient, due to the rapidly decaying exponent present in the integrand. For each value of the energy, we determined l for which the infinite sum in Eq. (10) could be considered converged. To assess the magnitude of the neglected terms, we used the Born approximation [19]

$$\tan\delta_l(E) \approx -2\mu_a k \int_0^\infty dR\, j_l^2(kR)V(R)R^2. \tag{75}$$

In our case, we assume the $-C_6/R^6$ asymptotic behavior of $V(R)$, which leads to

$$\tan\delta_l(E) \approx \frac{24\pi\mu_a^3 C_6 E^2}{(2l-3)(2l-1)(2l+1)(2l+3)(2l+5)}, \tag{76}$$

where $C_6 \approx 1.462$ is the total asymptotic coefficient (after summing BO, adiabatic, relativistic, and QED contributions). The numerical value of $\mu_a = \mu_n + 1$ was taken from the recent CODATA 18 database [11] (3648.149770710(120)m_e for helium-4 and 2748.942640035(120)m_e for helium-3. It must be noted that our interaction potential includes the retardation correction [22,57], which could suggest choosing the $-C_7/R^7$ long-range form. However, implementation of the retarding function in Eq. (75) would be cumbersome, so a simultaneously simpler and safer $-C_6/R^6$ assumption was made.

Note that the Born approximation is reliable when $l \gg l_{\text{lim}} \equiv R_{\text{ngl}}\sqrt{2\mu_a E}$, where R_{ngl} is the internuclear distance for
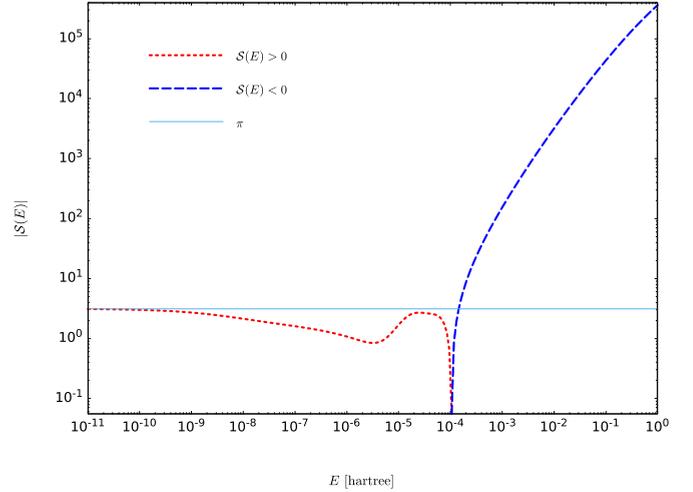
FIG. 1. Behavior of the function $\mathcal{S}(E)$ for helium-4 in the investigated energy range.

which the interaction potential can be considered negligible [19]. Because of that, the l summation was never stopped below l_{lim}. After testing different values, we chose $R_{\text{ngl}} = 150$ bohrs as a safe value for this purpose.

Equation (72) was propagated separately for each of the (E, l) pairs, with the potential function $V(R)$ described in Sec. III and $\mathcal{W}_\perp^{\text{int}}(R)$, $\mathcal{W}_\parallel^{\text{int}}(R)$, and $V_{\text{na}}^{\text{int}}(R)$ taken from Ref. [18]. We followed Ref. [15] in the choice of the integration step $\Delta R = 2 \times 10^{-5}E^{-1/3}$. Alternative choices were also tested, but we have observed no significant effect of choosing one over the other on the final results. Equations (24)–(26) were used to calculate the phase shifts. As the approximate phase shifts of Eqs. (25) and (26) do not have to be computed at every propagation step, they were tested at every $\lceil 2\pi/(\Delta R\sqrt{2\mu_a E})\rceil$th step (i.e., approximately once per wavelength). The propagation continued until a convergence criterion on the approximate phase shifts was met.

The shifts were combined with the help of Eq. (10) to obtain the $\mathcal{S}(E)$ function. Additionally, the $\mathcal{S}(0) = \pi$ point was added for helium-4 and $\mathcal{S}(0) = 0$ for helium-3, utilizing the Levinson theorem [19]. Quite interestingly, there are cases in the literature such as Ref. [14], which use interaction potentials "almost" supporting the bound state of helium-4 and manifest peculiar behavior of the $\mathcal{S}(E)$ function, which for $E \to 0$ appears to tend to π for helium-4, but then rapidly turns to zero. Our helium-4 $\mathcal{S}(E)$ curve is presented in Fig. 1. It is calculated with a potential which undoubtedly supports one bound state of $^4\text{He}_2$, so it correctly tends to π. The calculated $\mathcal{S}(E)$ values for both isotopes can be found in the Supplemental Material [56].

To calculate the second virial coefficient $B(T)$ from Eqs. (5)–(10), the obtained $\mathcal{S}(E)$ values were interpolated with third-order spline functions and numerically integrated, using the MATHEMATICA package [62]. The calculation was repeated with the uncertainty $\sigma(R)$ of the potential $V(R)$ added or subtracted from it, $V(R) \pm \sigma(R)$, to help estimate the final

TABLE II. Second virial coefficient $B(T)$ and second acoustic virial coefficient $\beta_a(T)$ for ⁴He (in $cm^3\ mol^{-1}$) calculated with our potential (B_{2020}, β_{2020}), compared to the data from Ref. [22] (B_{2012}, β_{2012}), for selected temperatures T (in K).

T	B_{2012}	σ_{2012}	B_{2020}	σ_{2020}	$\frac{\sigma_{2012}}{\sigma_{2020}}$	$\frac{B_{2020}-B_{2012}}{\sigma_{2012}}$	β_{2012}	σ_{2012}	β_{2020}	σ_{2020}	$\frac{\sigma_{2012}}{\sigma_{2020}}$	$\frac{\beta_{2020}-\beta_{2012}}{\sigma_{2012}}$
1.00	−475.74	0.37	−475.697	0.060	6.2	12%	−536.05	0.40	−536.004	0.067	6.0	11%
2.00	−194.38	0.13	−194.369	0.022	5.9	8%	−222.35	0.15	−222.339	0.025	6.0	8%
5.00	−64.302	0.042	−64.2979	0.0073	5.8	10%	−62.979	0.049	−62.9744	0.0085	5.8	9%
10.00	−23.125	0.020	−23.1230	0.0034	5.9	10%	−13.548	0.024	−13.5456	0.0040	6.0	10%
20.00	−2.7464	0.0097	−2.7453	0.0016	5.9	11%	10.224	0.012	10.2253	0.0020	6.1	11%
30.00	3.8382	0.0066	3.8390	0.0011	6.1	12%	17.4638	0.0083	17.4649	0.0013	6.3	13%
40.00	6.9768	0.0051	6.97747	0.00082	6.3	13%	20.6749	0.0064	20.67582	0.0010	6.4	14%
50.00	8.7506	0.0041	8.75111	0.00066	6.3	13%	22.3362	0.0053	22.33699	0.00080	6.6	15%
100.00	11.6747	0.0023	11.67507	0.00034	6.8	16%	24.2708	0.0030	24.27138	0.00042	7.1	19%
200.00	12.1644	0.0013	12.16462	0.00018	7.3	17%	23.2252	0.0017	23.22563	0.00023	7.6	25%
273.15	11.9279	0.0010	11.92814	0.00013	7.4	21%	22.2203	0.0013	22.22063	0.00017	7.6	25%
300.00	11.81919	0.00092	11.81940	0.00012	7.4	23%	21.8763	0.0012	21.87663	0.00016	7.6	27%
400.00	11.40110	0.00074	11.401282	0.000096	7.7	25%	20.73201	0.00099	20.73227	0.00012	8.0	26%
500.00	11.00715	0.00062	11.007306	0.000079	7.8	25%	19.77570	0.00084	19.77594	0.00010	8.1	28%
1000.00	9.55038	0.00037	9.550487	0.000045	8.3	29%	16.62467	0.00050	16.624815	0.000060	8.4	29%

uncertainty of $B(T)$. The total $B(T)$ error bar includes three sources of uncertainty, treated as uncorrelated:

(a) The first source is the error due to the numerical uncertainty $\sigma(R)$ of the potential $V(R)$, estimated as $(B_+(T) - B_-(T))/2$, where $B_\pm(T)$ denote the $B(T)$ values obtained with $V(R) \pm \sigma(R)$.

(b) The second source is the error due to interpolation, which was tested in two ways for each T: first, by increasing the order of the interpolating polynomial to 4, and second, by following the method proposed in Ref. [15], where the authors interpolated $S(k)$ (with $k = \sqrt{2\mu_a E}$) rather than $S(E)$, claiming that this method is more stable for small E. The larger of the two was taken as an estimate of the interpolation error. These effects were found to be small, less than 3% of the total uncertainty.

(c) The third source is the error due to finite accuracy of $S(E)$—less than 1% of the total σ for $T = 1$ K, but slowly rising to about 22% of the total error for the highest temperature considered. The uncertainty of $S(E)$ includes both the omitted summation terms from Eq. (10) and the error due to a finite propagation distance during the calculation of the phase shifts.

The potential-related uncertainty (a) dominates in the whole range of temperatures, the other two error sources being perceptible only for higher temperatures—and only because the potential-related one decays with T faster. An analogous error estimation procedure was applied to the acoustic coefficient $\beta_a(T)$, Eq. (11).

V. RESULTS AND SUMMARY

In Table II, selected values of the $B(T)$ and $\beta_a(T)$ coefficients computed by us for helium-4 are compared to those from Ref. [22]. Table III contains analogous data for helium-3. Data for more temperature values (including the 0.5–1.0 K range) are presented in the Supplemental Material [56]. The results are in agreement with those of Ref. [22]. However, due to the potential of a much better quality being used here, the uncertainty of both $B(T)$ and $\beta_a(T)$ has been

reduced by a significant factor for the whole investigated temperature range. The differences between new coefficients and those of Ref. [22] do not exceed 31% of the estimated σ_{2012} uncertainties from Ref. [22], showing that these errors were substantially overestimated. The possibility of this was pointed out to us by Gao and Pitre, based on their experimental work [63]. For low temperatures, the changes are below even the more stringent σ_{2020}.

As a by-product, the bound-state energy had to be calculated for helium-4. It was found to be −138.88(47) neV, confirming the value from the previous calculation [18].

For helium-4, calculations with particular $V(R)$ contributions turned on or off were performed to assess the significance of the adiabatic, retardation, and relativistic potential contributions to $B(T)$. The results are presented graphically in Fig. 2. In this context $\Delta B_{ad} = B(V_{BO} + V_{ad}) - B(V_{BO})$, $\Delta B_{rel} = B(V_{BO} + V_{ad} + V_{rel}) - B(V_{BO} + V_{ad})$, $\Delta B_{ret} = B(V_{ret}) - B(V_{BO})$ (where V_{ret} is V_{BO} with the $\sim 1/R^6$ term retarded [57]), and "total σ" is the uncertainty of $B(T)$. All these values were calculated with Eq. (17) with the reduced nuclear mass μ_n replaced with the reduced mass of two atoms, μ_a. The plot is consistent with Ref. [22], with the exception that the total uncertainty is now considerably reduced. Additionally, we tested the validity of using Eq. (17) with the atomic reduced mass instead of the nonadiabatic Eq. (18) in our proper calculations of $B(T)$ with the full potential $V(R)$. The difference $\Delta B_{nonad} = B(V) - B(V)_{at}$, where $B(V)_{at}$ is the result obtained with Eq. (17) with the atomic mass, is also shown in Fig. 2. It is considerably smaller than σ in the whole temperature range investigated. This can be explained by the fact that for helium, when R increases [18], the functions $\mu_\parallel(R)$ and $\mu_\perp(R)$ quickly reach values close to the reduced mass of two atoms, μ_a. It can also explain why ΔB_{nonad} rises slightly for higher temperatures: atoms with higher kinetic energy are able to penetrate the repulsive part of the interatomic potential deeper, where $\mu_\parallel(R)$ and $\mu_\perp(R)$ do have a nontrivial behavior. However, even for $T = 1000$ K this effect is almost six times smaller than the total uncertainty. Thus, it would be justified to use Eq. (17) with the atomic masses instead of the

TABLE III. Second virial coefficient $B(T)$ and second acoustic virial coefficient $\beta_a(T)$ for ^{3}He (in cm^3 mol^{-1}) calculated with our potential (B_{2020}, β_{2020}), compared to the data from Ref. [22] (B_{2012}, β_{2012}), for selected temperatures T (in K).

T	B_{2012}	σ_{2012}	B_{2020}	σ_{2020}	$\frac{\sigma_{2012}}{\sigma_{2020}}$	$\frac{B_{2020}-B_{2012}}{\sigma_{2012}}$	β_{2012}	σ_{2012}	β_{2020}	σ_{2020}	$\frac{\sigma_{2012}}{\sigma_{2020}}$	$\frac{\beta_{2020}-\beta_{2012}}{\sigma_{2012}}$
1.00	−236.39	0.19	−236.370	0.038	5.0	10%	−299.13	0.23	−299.107	0.044	5.2	10%
2.00	−130.882	0.094	−130.871	0.018	5.1	12%	−148.87	0.11	−148.858	0.021	5.2	11%
5.00	−47.368	0.036	−47.3636	0.0068	5.3	12%	−44.550	0.044	−44.5453	0.0080	5.5	11%
10.00	−16.200	0.018	−16.1975	0.0033	5.5	14%	−6.112	0.022	−6.1098	0.0039	5.6	10%
20.00	0.1061	0.0093	0.1071	0.0016	5.8	11%	13.281	0.012	13.2825	0.0019	6.2	13%
30.00	5.5362	0.0064	5.5370	0.0011	6.0	12%	19.2829	0.0081	19.2840	0.0013	6.2	13%
40.00	8.1519	0.0050	8.15248	0.00081	6.2	12%	21.9338	0.0063	21.93471	0.00099	6.4	14%
50.00	9.6336	0.0041	9.63419	0.00065	6.3	14%	23.2825	0.0052	23.28332	0.00080	6.5	16%
100.00	12.0385	0.0022	12.03883	0.00034	6.5	15%	24.6611	0.0029	24.66162	0.00042	6.9	18%
200.00	12.3144	0.0013	12.31464	0.00018	7.3	19%	23.3863	0.0017	23.38665	0.00023	7.6	21%
273.15	12.02871	0.00099	12.02892	0.00013	7.4	21%	22.3284	0.0013	22.32877	0.00017	7.6	28%
300.00	11.90860	0.00092	11.90880	0.00012	7.4	22%	21.9723	0.0012	21.97256	0.00016	7.6	22%
400.00	11.46304	0.00074	11.463209	0.000096	7.7	23%	20.79843	0.00099	20.79870	0.00012	8.0	27%
500.00	11.05373	0.00062	11.053881	0.000079	7.8	24%	19.82565	0.00084	19.82588	0.00010	8.1	27%
1000.00	9.56959	0.00037	9.569700	0.000045	8.3	30%	16.64527	0.00050	16.645422	0.000060	8.4	30%

more complicated Eq. (18) not only in this particular case, but probably even more so for heavier atoms, a practice done intuitively before.

Shortly after submission of this paper, a work [66] was published whose authors also perform calculations of the second virial and the second acoustic virial coefficient for helium-4 and helium-3. They employ the interatomic interaction potential from Ref. [18] (which our potential expands upon, as described in Sec. III). Their results for helium-4 agree with ours with respect to the assumed uncertainty, with comparable error bars. For helium-3 though, there is a substantial disagreement in the whole investigated temperature range. The authors of Ref. [66] themselves note the discrepancy with Ref. [22], which, in turn, is in perfect agreement with our results, as shown in Table III. It is difficult to pinpoint the cause of this disagreement with certainty. We note, however, that the potential from Ref. [18] was prepared specifically for helium-4 calculations, and its application to helium-3 requires

making certain manual changes in it, namely, rescaling the adiabatic contribution with the correct ^{4}He / ^{3}He nuclear mass ratio. There is no information in Ref. [66] whether it was corrected in such a way, and if not, it could—partially at least—lead to the observed difference in results. This would also explain why the results for helium-4 do agree. In fact, when neglecting this rescaling, we were able to obtain results for helium-3 consistent with Ref. [66] for temperatures greater than 7.5 K. The discrepancy for smaller temperatures remains, though, and its source remains unknown.

Although now the second virial coefficient is usually provided by the theory and used to interpret experimental data [5,6,10], not the other way around, there are some recent $B(T)$ measurements available [2,65]. Comparison of our $B(T)$ values with those experimental ones is presented in Table IV. One should note that the "experimental" values in this case are obtained by adding the theoretical second dielectric virial coefficient $b_\varepsilon(T)$ found in Ref. [64] to $B(T) - b_\varepsilon(T)$, which
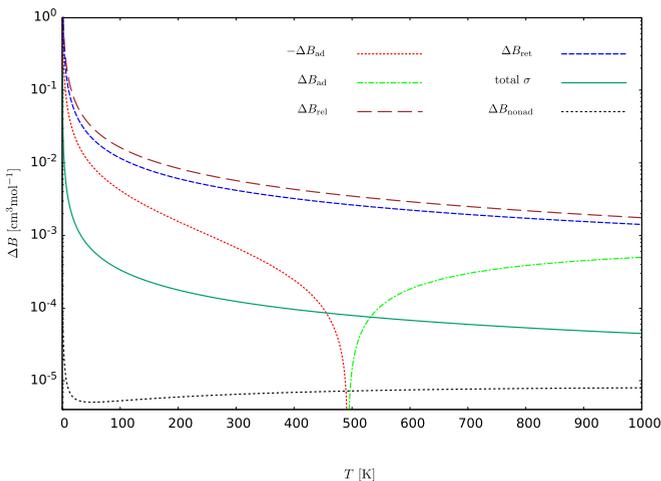
FIG. 2. Significance of potential contributions to the second virial coefficient $B(T)$ for helium-4 (in cm^3 mol^{-1}) compared to its uncertainty σ.

TABLE IV. Second virial coefficient $B(T)$ for ^{4}He (in cm^3 mol^{-1}), compared to the experimental data. Temperature T given in K. The subscript "th" denotes our theoretical results, "expt" the experimental ones, and $\Delta = B^{\text{th}} - B^{\text{expt}}$. All the experimental data are calculated by adding the dielectric virial coefficient $b_\varepsilon(T)$ found in Ref. [64] to the measured $B(T) - b_\varepsilon(T)$ from Ref. [65], except $T = 273.15$ K, where $B(T) - b_\varepsilon(T)$ is taken from Ref. [2].

T	B^{th}	σ^{th}	B^{expt}	σ^{expt}	Δ
5.00	−64.2979	0.0073	−64.147	0.068	−0.151
10.00	−23.1230	0.0034	−23.119	0.024	−0.004
20.00	−2.7453	0.0016	−2.734	0.038	−0.011
30.00	3.8390	0.0011	3.832	0.023	0.007
40.00	6.97747	0.00082	6.959	0.019	0.018
50.00	8.75111	0.00066	8.732	0.017	0.019
100.00	11.67507	0.00034	11.700	0.047	−0.025
200.00	12.16462	0.00018	12.22	0.21	−0.06
273.15	11.92814	0.00013	11.9258	0.0015	0.0023

TABLE V. Second acoustic virial coefficient $\beta_a(T)$ for ^{4}He (in cm^3 mol^{-1}), compared to the experimental data from Ref. [4]. Temperature T given in K. The subscript "th" denotes our theoretical results, "expt" the experimental ones [4], and $\Delta = \beta_a^{th} - \beta_a^{expt}$. For temperatures 273.1600 and 334.1700 K, there are several experimental results available.

T	β_a^{th}	σ^{th}	β_a^{expt}	σ^{expt}	Δ
235.1400	22.73307	0.00020	22.724	0.002	0.009
236.6190	22.71264	0.00019	22.710	0.003	0.003
247.0000	22.57027	0.00019	22.566	0.003	0.004
260.1200	22.39314	0.00018	22.386	0.002	0.007
273.1600	22.22050	0.00017	22.215	0.005	0.005
273.1600	22.22050	0.00017	22.216	0.001	0.004
273.1600	22.22050	0.00017	22.214	0.002	0.006
302.9146	21.84024	0.00016	21.841	0.004	−0.001
334.1700	21.46180	0.00014	21.459	0.002	0.003
334.1700	21.46180	0.00014	21.460	0.004	0.002
362.6000	21.13590	0.00013	21.138	0.004	−0.002
395.9000	20.77519	0.00013	20.773	0.004	0.002
396.2000	20.77204	0.00013	20.760	0.005	0.012
430.2400	20.42530	0.00012	20.416	0.012	0.009

is the actual quantity obtained from the experiment. Although the dielectric coefficients $b_\varepsilon(T)$ from Ref. [64] have been calculated in a semiclassical approximation only, substituting them with the quantum-statistical results from Refs. [67,68] yields no significant change. They are several orders of magnitude smaller than $B(T)$ and their uncertainty does not contribute to the error bar of these values. Our results agree with the experiment well, with only two outliers: a discrepancy of 2.2σ for 5 K and 1.6σ for 273.15 K.

Experimental values of the second acoustic virial coefficient $\beta_a(T)$ for helium-4 can be found in the Supplemental Material of Ref. [4]. In Table V, we compare them to our calculations. The degree of the agreement varies between different temperatures, as well as between different measurements for certain T. An explanation of this can be found in Ref. [4] itself: these values of $\beta_a(T)$ were obtained via a fit to an acoustic model, using all nine cavity

modes the measurement was performed for. On the other hand, the authors noted that the results for some of these acoustic modes are prone to errors—either due to an interference with the elastic resonances of the cavity shell or due to an overlap with neighboring modes—and discarded them from further analysis. However, as $\beta_a(T)$ is only an intermediate result in Ref. [4], it was not recalculated with such a refined data set. In their previous works, though, the authors of Ref. [4] used such constrained sets of acoustic modes when providing $\beta_a(T)$, albeit for one temperature only: $\beta_a(273.16 \text{ K}) = 22.2201(24) \text{ cm}^3 \text{ mol}^{-1}$ [69] and $22.2195(17) \text{ cm}^3 \text{ mol}^{-1}$ [70]. These results agree perfectly with each other, as well as with our value, $22.22050(17) \text{ cm}^3 \text{ mol}^{-1}$.

Analysis of the results leads to the conclusion that although our potential does not introduce any new physical effects if compared to its predecessor [18], it represents an improvement in the accuracy and reliability. The recalculated relativistic and QED components, as well as the augmented set of BO points used, not only ensure better justification of the uncertainty estimation but also give us a chance to present a bolder, more stringent one. Hopefully, it should meet the demands of constantly developing experimental metrology in the foreseeable future, as well as constitute the next step forward on the path to a new pressure standard.

[1] C. Gaiser, T. Zandt, and B. Fellmuth, Metrologia **52**, S217 (2015).

[2] C. Gaiser and B. Fellmuth, J. Chem. Phys. **150**, 134303 (2019).

[3] M. R. Moldover, R. M. Gavioso, J. B. Mehl, L. Pitre, M. de Podesta, and J. Zhang, Metrologia **51**, R1 (2014).

[4] R. M. Gavioso, D. M. Ripa, P. P. M. Steur, R. Dematteis, and D. Imbraguglio, Metrologia **56**, 045006 (2019).

[5] B. Gao, L. Pitre, E. C. Luo, M. D. Plimmer, P. Lin, J. T. Zhang, X. J. Feng, Y. Y. Chen, and F. Sparasci, Measurement **103**, 258 (2017).

[6] B. Gao, H. Y. Zhang, D. X. Han, C. Z. Pan, H. Chen, Y. N. Song, W. J. Liu, J. F. Hu, X. J. Kong, F. Sparasci *et al.*, Metrologia, doi:10.1088/1681-7575/ab84ca.

[7] P. M. C. Rourke, C. Gaiser, B. Gao, D. M. Ripa, and M. R. Moldover, Metrologia **56**, 032001 (2019).

[8] J. W. Schmidt, R. M. Gavioso, E. F. May, and M. R. Moldover, Phys. Rev. Lett. **98**, 254504 (2007).

[9] J. Hendricks, Nat. Phys. **14**, 100 (2018).

[10] C. Gaiser, B. Fellmuth, and W. Sabuga, Nat. Phys. **16**, 177 (2020).

[11] E. Tiesinga, P. J. Mohr, D. B. Newell, and B. N. Taylor, *The 2018 CODATA Recommended Values of the Fundamental Physical Constants* (Web version 8.1), http://physics.nist.gov/constants

[12] A. D. Buckingham and J. A. Pople, Trans. Faraday Soc. **51**, 1029 (1955).

[13] J. E. Kilpatrick, J. Chem. Phys. **21**, 274 (1953).

[14] J. E. Kilpatrick, W. E. Keller, E. F. Hammel, and N. Metropolis, Phys. Rev. **94**, 1103 (1954).

[15] J. J. Hurly and J. B. Mehl, J. Res. Natl. Inst. Stand. Technol. **112**, 75 (2007).

[16] K. Pachucki and J. Komasa, J. Chem. Phys. **129**, 034102 (2008).

[17] K. Pachucki and J. Komasa, J. Chem. Phys. **143**, 034111 (2015).

[18] M. Przybytek, W. Cencek, B. Jeziorski, and K. Szalewicz, Phys. Rev. Lett. **119**, 123401 (2017).

[19] C. J. Joachain, *Quantum Collision Theory* (North-Holland, Amsterdam, 1975).

[20] H. Piel and M. Chrysos, Mol. Phys. **116**, 2364 (2018).

[21] N. Levinson, K. Dan. Vidensk. Selsk. Mat.-Fys. Medd. **25** (1949).

[22] W. Cencek, M. Przybytek, J. Komasa, J. B. Mehl, B. Jeziorski, and K. Szalewicz, J. Chem. Phys. **136**, 224303 (2012).

[23] W. Kutzelnigg, Mol. Phys. **90**, 909 (1997).

[24] N. C. Handy, Y. Yamaguchi, and H. F. Schaefer III, J. Chem. Phys. **84**, 4481 (1986).

[25] A. G. Ioannou, R. D. Amos, and N. C. Handy, Chem. Phys. Lett. **251**, 52 (1996).

[26] N. C. Handy and A. M. Lee, Chem. Phys. Lett. **252**, 425 (1996).

[27] J. Gauss, A. Tajti, M. Kállay, J. F. Stanton, and P. G. Szalay, J. Chem. Phys. **125**, 144111 (2006).

[28] A. Tajti, P. G. Szalay, and J. Gauss, J. Chem. Phys. **127**, 014102 (2007).

[29] M. Przybytek, W. Cencek, J. Komasa, G. Łach, B. Jeziorski, and K. Szalewicz, Phys. Rev. Lett. **104**, 183003 (2010).

[30] H. A. Bethe and E. E. Salpeter, *Quantum Mechanics of One- and Two-Electron Atoms* (Springer, Berlin, 1957).

[31] R. D. Cowan and D. C. Griffin, J. Opt. Soc. Am. **66**, 1010 (1976).

[32] H. Araki, Prog. Theor. Phys. **17**, 619 (1957).

[33] J. Sucher, Phys. Rev. **109**, 1010 (1958).

[34] K. Pachucki, J. Phys. B **31**, 5123 (1998).

[35] K. Piszczatowski, G. Lach, M. Przybytek, J. Komasa, K. Pachucki, and B. Jeziorski, J. Chem. Theory Comput. **5**, 3039 (2009).

[36] V. I. Korobov, Phys. Rev. A **69**, 054501 (2004).

[37] G. W. F. Drake, Nucl. Instrum. Methods Phys. Res. B **31**, 7 (1988).

[38] S. Coriani, T. Helgaker, P. Jørgensen, and W. Klopper, J. Chem. Phys. **121**, 6591 (2004).

[39] S. Boys and F. Bernardi, Mol. Phys. **19**, 553 (1970).

[40] K. Aidas, C. Angeli, K. L. Bak, V. Bakken, R. Bast, L. Boman, O. Christiansen, R. Cimiraglia, S. Coriani, P. Dahle *et al.*, WIREs Comput. Mol. Sci. **4**, 269 (2014).

[41] DALTON, a molecular electronic structure program, release 2013.2 (2013), http://daltonprogram.org

[42] M. Przybytek (2014), general FCI program HECTOR.

[43] DALTON, a molecular electronic structure program, release 2.0 (2005), http://daltonprogram.org

[44] J. G. Balcerzak, M. Lesiuk, and R. Moszynski, Phys. Rev. A **96**, 052510 (2017).

[45] M. Lesiuk and B. Jeziorski, J. Chem. Theory Comput. **15**, 5398 (2019).

[46] W. Kutzelnigg, Int. J. Quantum Chem. **108**, 2280 (2008).

[47] M. Przybytek and B. Jeziorski, Chem. Phys. **401**, 170 (2012).

[48] W. J. Meath and J. O. Hirschfelder, J. Chem. Phys. **44**, 3197 (1966).

[49] R. A. Sack, J. Math. Phys. **5**, 260 (1964).

[50] J.-Y. Zhang, Z.-C. Yan, D. Vrinceanu, J. F. Babb, and H. R. Sadeghpour, Phys. Rev. A **74**, 014704 (2006).

[51] K. T. Tang and J. P. Toennies, J. Chem. Phys. **80**, 3726 (1984).

[52] L.-Y. Tang, Z.-C. Yan, T.-Y. Shi, and J. Mitroy, Phys. Rev. A **84**, 052502 (2011).

[53] M. Przybytek and B. Jeziorski, Chem. Phys. Lett. **459**, 183 (2008).

[54] M. Puchalski, J. Komasa, and K. Pachucki, Phys. Rev. A **87**, 030502(R) (2013).

[55] *Handbook of Atomic, Molecular, and Optical Physics*, edited by G. W. F. Drake (Springer, Berlin, 2006).

[56] See Supplemental Material at http://link.aps.org/supplemental/10.1103/PhysRevA.102.042810 for the calculated values of the interaction potential contributions, Fortran implementation of the potential, values of the virial and acoustic virial coefficients for a larger set of temperatures, and calculated values of the $\mathcal{S}(E)$ function.

[57] M. Przybytek, B. Jeziorski, W. Cencek, J. Komasa, J. B. Mehl, and K. Szalewicz, Phys. Rev. Lett. **108**, 183201 (2012).

[58] B. Numerov, Trudy Glavnoi rossiiskoi astrofizicheskoi observatorii **2**, 188 (1923).

[59] J. M. Blatt, J. Comput. Phys. **1**, 382 (1967).

[60] J. P. Leroy and R. Wallace, J. Comput. Phys. **67**, 239 (1986).

[61] B. R. Johnson, J. Chem. Phys. **67**, 4086 (1977).

[62] MATHEMATICA, version 7.0.1.0 (Wolfram Research, Inc., Champaign, IL, 2009).

[63] B. Gao and L. Pitre (private communication).

[64] B. Song and Q.-Y. Luo, Metrologia **57**, 025007 (2020).

[65] C. Gaiser and B. Fellmuth, Metrologia (to be published).

[66] B. Song, P. Xu, and M. He, Mol. Phys. (2020), doi:10.1080/00268976.2020.1802525.

[67] G. Garberoglio and A. H. Harvey, J. Res. Natl. Inst. Stand. Technol. **125**, 125022 (2020).

[68] A. H. Harvey and G. Garberoglio, Calculated Values of the Second Dielectric and Refractivity Virial Coefficients of Helium, Neon, and Argon (NIST, Gaithersburg, MD, 2020).

[69] R. M. Gavioso, G. Benedetto, D. M. Ripa, P. A. G. Albo, C. Guianvarc'h, A. Merlone, L. Pitre, D. Truong, F. Moro, and R. Cuccaro, Int. J. Thermophys. **32**, 1339 (2011).

[70] R. M. Gavioso, D. M. Ripa, P. P. M. Steur, C. Gaiser, D. Truong, C. Guianvarc'h, P. Tarizzo, F. M. Stuart, and R. Dematteis, Metrologia **52**, S274 (2015).